



Fermi National Accelerator Laboratory

FERMILAB-PUB-94/074-T

NUHEP-TH-94-6

March 1994

***J/ψ* Production from  
Electromagnetic Fragmentation  
in  $Z^0$  decay**

Sean Fleming

*Department of Physics and Astronomy*

*Northwestern University, Evanston, IL 60208*

and

*Fermi National Accelerator Laboratory*

*P.O. Box 500, Batavia, IL 60510*

**Abstract**

The rate for  $Z^0 \rightarrow J/\psi + \ell^+ \ell^-$  is surprisingly large with about one event for every million  $Z^0$  decays. The reason for this is that there is a fragmentation contribution that is not suppressed by a factor of  $M_\psi^2/M_Z^2$ . In the fragmentation limit  $M_Z \rightarrow \infty$  with  $E_\psi/M_Z$  fixed, the differential decay rate for  $Z^0 \rightarrow J/\psi + \ell^+ \ell^-$  factors into electromagnetic decay rates and universal fragmentation functions. The fragmentation functions for lepton fragmentation and photon fragmentation into  $J/\psi$  are calculated to lowest order in  $\alpha$ . The fragmentation approximation to the rate is shown to match the full calculation for  $E_\psi$  greater than about  $3M_\psi^2$ .



## Introduction

Fragmentation is the decay of a high transverse momentum parton into a collinear hadron. The differential cross section for the inclusive production of such a hadron in  $e^+e^-$  annihilation factors into differential cross sections  $d\hat{\sigma}$  for the production of large transverse momentum partons and fragmentation functions  $D(z)$  [1]. The fragmentation function gives the probability for the splitting of a parton into the hadron with momentum fraction  $z$ . These functions are independent of the subprocess that creates the fragmenting particle, and can be evolved to any scale via the Altarelli-Parisi evolution equations.

It has recently been shown that it is possible to calculate the fragmentation functions for heavy quarkonium states using perturbative quantum chromodynamics (QCD) [2]. Fragmentation functions for several of these states have been calculated explicitly [2, 3, 4, 5, 6]. In particular the paper of Braaten, Chueng and Yuan on charm quark fragmentation [3] is most relevant to the work presented here. Their analysis focuses on decays of the  $Z^0$  into hadrons showing that charmonium production is dominated by charm quark fragmentation. In an analagous manner it is shown here that decays of the  $Z^0$  into charmonium plus electromagnetic particles (leptons and photons) are dominated by electromagnetic fragmentation.

The process  $Z^0 \rightarrow \psi + \ell^+\ell^-$ , which is of order  $\alpha^2$ , where  $\alpha$  is the electromagnetic coupling constant, has a branching ratio of  $7.5 \times 10^{-7}$ . This is an order of magnitude larger than the order- $\alpha$  process  $Z^0 \rightarrow \psi\gamma$  [7], which has a branching ratio of  $5.2 \times 10^{-8}$ . That makes  $Z^0 \rightarrow \psi + \ell^+\ell^-$  the dominant  $\psi$  production mechanism in electromagnetic  $Z^0$  decays. The unexpectedly large rate can be explained by a fragmentation contribution which is not suppressed by a factor of  $M_\psi^2/M_Z^2$  [2]. In this paper, it is shown that in the fragmentation limit  $M_Z \rightarrow \infty$  with  $E_\psi/M_Z$  fixed, the rate for  $Z^0 \rightarrow \psi + \ell^+\ell^-$  factors into subprocess rates for electromagnetic decays and individual fragmentation functions. At leading order in  $\alpha$  there is a contribution from the fragmentation function  $D_{\ell \rightarrow \psi}$  for a lepton to split into a  $\psi$ , and a contribution from the fragmentation function  $D_{\gamma \rightarrow \psi}$  for a photon to split into a  $\psi$ . The fragmentation functions are calculated in a manner that is independent of the hard process that produces the fragmenting parton, and the fragmentation calculation is shown to match the full calculation for  $E_\psi$  greater than about  $3M_\psi$ .

### The decay rate for $Z^0 \rightarrow \psi + \ell^+ \ell^-$

The decay rate for  $Z^0 \rightarrow \psi + \ell^+ \ell^-$  was calculated in a model-independent way in Ref. [8, 9] using the Feynman diagrams in figure 1a. The diagrams in figure 1b also contribute to this process at the same order in the electromagnetic coupling  $\alpha$ . Fortunately they can be neglected.

In order to understand why only the diagrams of figure 1a need to be considered it is necessary to understand why the rate for  $Z^0 \rightarrow \psi \gamma$  is smaller than the rate for  $Z^0 \rightarrow \psi + \ell^+ \ell^-$ . Naively one would expect  $\Gamma(Z^0 \rightarrow \psi \gamma)$  to be larger than  $\Gamma(Z^0 \rightarrow \psi + \ell^+ \ell^-)$  since the latter rate is suppressed by a power of  $\alpha$  compared to the former rate. However upon closer examination this expectation turns out to be untrue. To see why compare the diagrams that contribute to the decay rates  $\Gamma(Z^0 \rightarrow \psi + \ell^+ \ell^-)$  figure 1 and  $\Gamma(Z^0 \rightarrow \psi \gamma)$  figure 2. It is important to note that the lepton propagator in the diagrams of figure 2 is always of order  $1/M_Z^2$ . In contrast there is a substantial region of phase space where both the photon propagator and the lepton propagator in the diagrams of figure 1a are of order  $1/M_\psi^2$ . Thus these diagrams will be enhanced by a factor of  $M_Z^2/M_\psi^2$ , compared to the diagrams of figure 2. The factor of  $M_Z^2/M_\psi^2$  is large enough to overwhelm the extra power of  $\alpha$  making the diagrams of figure 1a more important than the diagrams of figure 2. The lepton propagator of the diagrams in figure 1b is always of order  $1/M_Z^2$ , so these diagrams are suppressed by a factor of  $\alpha$  compared to the diagrams in figure 2, and may be neglected.

The remaining diagrams that contribute to  $\Gamma(Z^0 \rightarrow \psi + \ell^+ \ell^-)$  at the same order in  $\alpha$  are obtained from the diagrams of figure 1 by replacing the photon propagator with a  $Z$ -boson. Then the boson propagator in the diagrams of figure 1a is always of order  $1/M_Z^2$ . Similarly the lepton propagator in the diagrams of figure 1b is also always of order  $1/M_Z^2$ . Thus these diagrams are suppressed by a factor of  $\alpha$  compared to the diagrams of figure 2 and can be neglected.

Keeping only the diagrams in figure 1a, and neglecting the lepton mass, the result of

the calculation of  $\Gamma(Z^0 \rightarrow \psi + \ell^+ \ell^-)$  is

$$\Gamma = 4\alpha^2 g_\psi^2 \Gamma(Z^0 \rightarrow \ell^+ \ell^-) \int_{2\sqrt{\lambda}}^{1+\lambda} dy \int_{-\sqrt{y^2-4\lambda}}^{\sqrt{y^2-4\lambda}} dw g(y, w, \lambda)$$

$$g(y, w, \lambda) = \frac{1}{2} \left( \frac{(y-2)^2 + w^2}{y^2 - w^2} \right) - 2\lambda \left( \frac{2w^2 - (y^2 - w^2)(1-y)}{(y^2 - w^2)^2} \right) + 2\lambda^2 \left( \frac{1}{y^2 - w^2} \right) \quad (1)$$

where  $\lambda = M_\psi^2/M_Z^2$ ,  $y = 2P \cdot Z/M_Z^2$  and  $w = 2(p_+ - p_-) \cdot Z/M_Z^2$ . Here  $P$ ,  $p_-$ ,  $p_+$ , and  $Z$  are the 4-momenta of the  $\psi$ ,  $\ell^-$ ,  $\ell^+$ , and  $Z^0$ . The parameter  $g_\psi$  can be determined from the electronic width  $\Gamma_{e^+e^-}$  of the  $\psi$  to be

$$g_\psi^2 = \frac{3}{4\pi} \frac{\Gamma_{e^+e^-}}{\alpha^2 M_\psi}. \quad (2)$$

Using  $\Gamma_{e^+e^-} = 5.4$  keV the photon-to- $\psi$  coupling is  $g_\psi^2 = 0.008$ . Integrating the function  $g(y, w, \lambda)$  over  $w$  yields the full differential decay rate

$$\frac{d\Gamma}{dE_\psi} = 8\alpha^2 g_\psi^2 \frac{\Gamma(Z^0 \rightarrow \ell^+ \ell^-)}{M_Z} \left[ \left( \frac{(y-1)^2 + 1}{y} + \lambda \frac{3-2y}{y} + \lambda^2 \frac{2}{y} \right) \log \frac{y+y_L}{y-y_L} - 2y_L \right], \quad (3)$$

where  $y_L = \sqrt{y^2 - 4\lambda}$ . In the center of mass frame  $y = 2E_\psi/M_Z$ . Later on these results will be compared to the fragmentation calculation in the fragmentation limit  $M_Z \rightarrow \infty$  with  $E_\psi/M_Z$  fixed. In this limit Eq. (3) reduces to

$$\frac{d\Gamma}{dE_\psi} = 8\alpha^2 g_\psi^2 \frac{\Gamma(Z^0 \rightarrow \ell^+ \ell^-)}{M_Z} \left[ \frac{(y-1)^2 + 1}{y} \log \frac{y^2}{\lambda} - 2y \right]. \quad (4)$$

### The Fragmentation Contribution to $Z^0$ Decay

In reference [3] the general form of the fragmentation contribution for the production of a  $\psi$  of energy  $E_\psi$  in  $Z^0$  decays is given as

$$d\Gamma(Z^0 \rightarrow \psi(E_\psi) + X) = \sum_i \int dz d\hat{\Gamma}(Z^0 \rightarrow i(E_\psi/z) + X, \mu^2) D_{i \rightarrow \psi}(z, \mu^2), \quad (5)$$

where the sum is over partons and  $z$  is the longitudinal momentum fraction of the  $\psi$  relative to the fragmenting parton. All of the dependence on the  $\psi$  energy  $E_\psi$  has been factored into the subprocess decay rate  $\hat{\Gamma}$  and all of the dependence on the  $\psi$  mass  $M_\psi$  has been factored into the fragmentation function  $D_{i\rightarrow\psi}(z, \mu^2)$ . A factorization scale  $\mu$  has to be introduced in order to maintain this factored form in all orders of perturbation theory. This general form was developed in the context of QCD, but it applies equally to QED, where the only partons are leptons and photons. This simplifies the general electromagnetic fragmentation contribution to

$$\begin{aligned} \frac{d\Gamma}{dE_\psi}(Z^0 \rightarrow \psi(E_\psi) + X) = & \\ & 2 \int_0^1 dz \int dE_\ell \frac{d\hat{\Gamma}}{dE_\ell}(Z^0 \rightarrow \ell^-(E_\ell) + X, \mu^2) D_{\ell\rightarrow\psi}(z, \mu^2) \delta(E_\psi - zE_\ell) \\ & + \int_0^1 dz \int dE_\gamma \frac{d\hat{\Gamma}}{dE_\gamma}(Z^0 \rightarrow \gamma(E_\gamma) + X, \mu^2) D_{\gamma\rightarrow\psi}(z, \mu^2) \delta(E_\psi - zE_\gamma), \end{aligned} \quad (6)$$

where  $X$  are electromagnetic final states, and  $E_\ell$  and  $E_\gamma$  are the lepton and photon energies. The factor of 2 accounts for the fragmentation contribution from both the  $\ell^-$  and the  $\ell^+$ . Large logarithms of  $E_\psi/\mu$  in the subprocess decay rate  $\hat{\Gamma}$  can be avoided by choosing  $\mu$  on the order of  $E_\psi$ . The large logarithms of order  $E_\psi/M_\psi$  which then appear in the fragmentation functions can be summed up by solving the Altarelli-Parisi evolution equation. In the electromagnetic case the evolution of the fragmentation functions is of order  $\alpha$  and may be neglected.

It is easy to count the order of  $\alpha$  for the leading order fragmentation contributions to Eq. (6). The subprocess rate for  $Z^0 \rightarrow \ell^- + X$  is of order 1, while the subprocess rate for  $Z^0 \rightarrow \gamma + X$  is of order  $\alpha$ . The fragmentation function for a lepton to split into a  $\psi$  will be shown to be of order  $\alpha^2$ , while the fragmentation function for a photon to split into a  $\psi$  will be shown to be of order  $\alpha$ . Therefore both fragmentation processes will contribute to Eq. (6) at leading order in  $\alpha$ .

At lowest order in  $\alpha$  it is possible to simplify things. The energy distribution for the

subprocess  $Z^0 \rightarrow \ell^-(E_\ell) + X$  at lowest order is

$$\frac{d\hat{\Gamma}}{dE_\ell} = \hat{\Gamma}(Z^0 \rightarrow \ell^+\ell^-) \delta(E_\ell - \frac{M_Z}{2}). \quad (7)$$

Furthermore the photon fragmentation function at lowest order can be written as

$$D_{\gamma \rightarrow \psi}(z, \mu^2) = P_{\gamma \rightarrow \psi} \delta(z - 1) \quad (8)$$

where the function  $P_{\gamma \rightarrow \psi}$  is the probability for a photon to split into a  $\psi$ , and  $z$  is the longitudinal momentum fraction of the  $\psi$  relative to the  $\gamma$ . These simplifications reduce the fragmentation contribution to the energy distribution Eq. (6) at leading order in  $\alpha$  to:

$$\begin{aligned} \frac{d\Gamma}{dE_\psi}(Z^0 \rightarrow \psi(E_\psi) + \ell^+\ell^-) = \\ \frac{4}{M_Z} \hat{\Gamma}(Z^0 \rightarrow \ell^+\ell^-) D_{\ell \rightarrow \psi}(\frac{2E_\psi}{M_Z}, \mu^2) + \frac{d\hat{\Gamma}}{dE_\psi}(Z^0 \rightarrow \gamma(E_\psi) + \ell^+\ell^-, \mu^2) P_{\gamma \rightarrow \psi}. \end{aligned} \quad (9)$$

The physical interpretation of the first term on the right hand side of Eq. (9) is that the  $Z^0$  decays into two leptons, with energies  $M_Z/2$  on a distance scale of order  $1/M_Z$ . Subsequently one of the leptons decays into a collinear lepton and  $\psi$  on a distance scale of order  $1/M_\psi$ . The physical interpretation of the second term is that the  $Z^0$  decays into two leptons and a photon with energy  $E_\psi$  on a distance scale of order  $1/M_Z$ , and the photon fragments into a  $\psi$  on a distance scale of order  $1/M_\psi$ . Note that at this order the only dependence on the factorization scale is in  $D_{\ell \rightarrow \psi}$  and in the subprocess rate for  $Z^0 \rightarrow \gamma + \ell^+\ell^-$ .

Given the general form of the fragmentation contribution at lowest order in  $\alpha$  in Eq. (9), it is only necessary to calculate the fragmentation function  $D_{\ell \rightarrow \psi}(z, \mu^2)$ , the fragmentation probability  $P_{\gamma \rightarrow \psi}$ , and the subprocess rate for the  $Z^0 \rightarrow \gamma + \ell^+\ell^-$ .

### Photon Fragmentation

The fragmentation function  $D_{\gamma \rightarrow \psi}(z, \mu^2)$  for a photon to split into a  $\psi$  can be calculated in a manner that is independent of the process that produces the fragmenting photon. The Feynman diagram in figure 3a represent such a process at lowest order in  $\alpha$ . An unknown vertex, represented by the circle, radiates a photon which fragments into a  $\psi$ . The

fragmentation probability  $P_{\gamma \rightarrow \psi}$  can be isolated by dividing the cross section  $\sigma_1$ , for the production of a  $\psi$  with energy  $E_\psi$ , by the cross section  $\sigma_0$ , for the production of a real photon of energy  $E_\gamma = E_\psi$ , in the limit  $E_\psi \gg M_\psi$  where fragmentation dominates.

The general form of the photon production cross section  $\sigma_0$  is

$$\sigma_0 = \frac{1}{Flux} \int [dk][dp_{out}] (2\pi)^4 \delta^4(p_{in} - k - p_{out}) \sum |A_0|^2 \quad (10)$$

where  $p_{in}$  is the sum of incoming 4-momenta,  $k$  is the photon 4-momentum, and  $p_{out}$  is the sum of the remaining outgoing 4-momenta. Here  $[dk] = d^3k/(16\pi^3k_0)$  is the Lorentz-invariant phase space for the photon and  $[dp_{out}]$  is the Lorentz invariant phase space for the remaining outgoing particles,  $Flux$  denotes the incoming particle flux for which no explicit expression is needed since it will cancel the same factor when  $\sigma_1$  is divided by  $\sigma_0$ . The amplitude  $A_0$  for the process can be calculated from the Feynman diagram in figure 3b

$$A_0 = \Gamma^\mu \epsilon_\mu, \quad (11)$$

where  $\Gamma^\mu$  is a vertex factor for the production of the photon, for which the explicit form is not needed. Squaring and summing over final spins gives

$$\sum |A_0|^2 = -\Gamma^\mu \Gamma_\mu^*. \quad (12)$$

The general form of the  $\gamma \rightarrow \psi$  cross section  $\sigma_1$  is

$$\sigma_1 = \frac{1}{Flux} \int [dP][dp_{out}] (2\pi)^4 \delta^4(p_{in} - P - p_{out}) \sum |A_1|^2 \quad (13)$$

where  $P$  is the  $\psi$  4-momentum.  $Flux$ ,  $p_{in}$ , and  $p_{out}$  are the same as described after Eq. (10). The amplitude  $A_1$  can be calculated from the Feynman diagram in figure 3a

$$A_1 = \frac{g_\psi e}{4} \Gamma^\mu (-g_{\mu\nu}) \text{tr}[\not{\epsilon} \not{\gamma}^\nu], \quad (14)$$

where  $\epsilon$  is the  $\psi$  polarization vector, and  $\Gamma^\mu$  is the vertex factor for the production of a virtual photon with invariant mass  $M_\psi$ . Squaring the amplitude and summing over final spins gives

$$\sum |A_1|^2 = -4\pi g_\psi^2 \alpha \Gamma^\mu \Gamma_\mu^* \quad (15)$$

The vertex factor  $\Gamma^\mu$  in Eq. (14) only differs from the vertex factor in Eq. (11) in one respect, it is evaluated at the point  $k^2 = M_\psi^2$  instead of  $k^2 = 0$ . Aside from the vertex factor the  $\psi$  mass enters the cross section  $\sigma_1$  in the phase space integral. The contribution to photon fragmentation will come from a region of phase space where  $E_\psi \gg M_\psi$  so that the  $\psi$  mass can be neglected. Then the cross section  $\sigma_1$  can be written as

$$\sigma_1 = 4\pi g_\psi^2 \alpha \sigma_0. \quad (16)$$

The fragmentation probability  $P_{\gamma \rightarrow \psi}$  can be read off from Eq.(16):

$$P_{\gamma \rightarrow \psi} = 4\pi g_\psi^2 \alpha. \quad (17)$$

Evaluating this numerically gives a fragmentation probability of  $P_{\gamma \rightarrow \psi} = 7 \times 10^{-4}$ .

### Photon Subprocess

The energy distribution of the subprocess  $Z^0 \rightarrow \gamma + \ell^+ \ell^-$  is calculated next. At this point it is necessary to decide what part of the  $Z^0 \rightarrow \psi + \ell^+ \ell^-$  phase space is to be identified as photon fragmentation, and what part is interpreted as lepton fragmentation. In Eq. (9), the dependence on the factorization scale  $\mu$  cancels between  $D_{\ell \rightarrow \psi}$  and  $d\hat{\Gamma}/dE_\psi$ . Thus by changing  $\mu$  some of the lepton fragmentation contribution can be moved into the photon fragmentation term and vice versa. There is therefore no clear crossover from lepton fragmentation to photon fragmentation, which makes it necessary to make an arbitrary choice on the appropriate phase space cutoff. In this paper a cutoff on the invariant mass of the  $\ell - \psi$  system, where  $\ell$  is the fragmenting lepton, is introduced. The contribution to the differential decay rate from negative lepton fragmentation is considered to come from the region of phase space where  $s < \mu^2$ . Here  $s$  is the invariant mass of the  $\ell^- - \psi$  system. Similarly the contribution from positive lepton fragmentation is considered to come from the region  $s' < \mu^2$  where  $s'$  is the invariant mass of the  $\ell^+ - \psi$  system. The photon fragmentation contribution is interpreted as coming from the remaining region. In the calculation of the photon subprocess the invariant-mass cutoffs translate into a limit on the phase space of the photon energy distribution.

The decay rate for  $Z^0 \rightarrow \gamma + \ell^+ \ell^-$  is

$$\Gamma(Z^0 \rightarrow \gamma + \ell^+ \ell^-) = \frac{1}{2M_Z} \int [dk][dp_+][dp_-] (2\pi)^4 \delta^4(Z - k - p_+ - p_-) \frac{1}{3} \sum |A|^2, \quad (18)$$

where  $k$ ,  $p_+$ ,  $p_-$  and  $Z$  are the 4-momenta of the photon,  $\ell^+$ ,  $\ell^-$ , and  $Z^0$ . The amplitude can be calculated from the diagrams in figure 4. Averaging over initial spins and summing over final spins reduces the square of the amplitude to

$$\frac{1}{3} \sum |A|^2 = \frac{g_w^2 e^2}{6 \cos^2 \theta_w} (C_V^2 + C_A^2) \frac{(y-2)^2 + w^2}{y^2 - w^2} \quad (19)$$

where  $y = 2k \cdot Z/M_Z^2$ , and  $w = 2(p_+ - p_-) \cdot Z/M_Z^2$ ,  $C_V = -1 + 4 \sin^2 \theta_w$  and  $C_A = 1$ ,  $g_w$  is the weak coupling constant, and  $\theta_w$  is the weak mixing angle. Note that aside from the normalization this is the same as the integrand of Eq. (1) in the limit  $M_\psi \rightarrow 0$ . Simplifying the phase space integral, Eq. (18) reduces to

$$\Gamma(Z^0 \rightarrow \gamma + \ell^+ \ell^-) = \frac{M_Z}{32(2\pi)^3} \int_{2\mu^2/M_Z^2}^1 dy \int_{-(y-2\mu^2/M_Z^2)}^{(y-2\mu^2/M_Z^2)} dw \frac{1}{3} \sum |A|^2, \quad (20)$$

where the limits on the invariant masses  $s$  and  $s'$  translate into the limits on  $w$ . Integrating over  $w$  gives the photon energy distribution in the decay  $Z^0 \rightarrow \gamma + \ell^+ \ell^-$ :

$$\begin{aligned} \frac{d\hat{\Gamma}}{dE_\gamma}(Z^0 \rightarrow \gamma(E_\gamma) + \ell^+ \ell^-, \mu^2) = \\ \frac{2\alpha}{\pi} \frac{\Gamma(Z^0 \rightarrow \ell^+ \ell^-)}{M_Z} \left[ \frac{(y-1)^2 + 1}{y} \log \left( \frac{y - \mu^2/M_Z^2}{\mu^2/M_Z^2} \right) - y + 2 \frac{\mu^2}{M_Z^2} \right] \theta(y - \frac{2\mu^2}{M_Z^2}), \end{aligned} \quad (21)$$

where  $y = 2E_\gamma/M_Z$ . It is possible to simplify the expression for the energy distribution by taking the limit  $\mu \ll M_Z$ . In this limit Eq. (21) simplifies to

$$\frac{d\hat{\Gamma}}{dE_\gamma}(Z^0 \rightarrow \gamma(E_\gamma) + \ell^+ \ell^-, \mu^2) = \frac{2\alpha}{\pi} \frac{\Gamma(Z^0 \rightarrow \ell^+ \ell^-)}{M_Z} \left[ \frac{(y-1)^2 + 1}{y} \log \frac{yM_Z^2}{\mu^2} - y \right]. \quad (22)$$

The price that is paid for this simplification is that smooth threshold behavior at  $y = 2\mu^2/M_Z^2$  is lost, and the differential decay rate becomes negative at sufficiently small values of  $y$ . Since

the fragmentation approximation breaks down in the threshold region anyway nothing is lost by making this simplification.

### Lepton Fragmentation

The calculation of the fragmentation function  $D_{\ell \rightarrow \psi}(z, \mu^2)$  for a lepton to split into a  $\psi$  parallels that of the photon fragmentation function. At leading order in  $\alpha$  the process is symbolically represented by the diagram in figure 5a. The fragmentation probability is obtained by dividing  $\sigma_1$ , the cross section for the production of  $\psi + \ell^-$ , by  $\sigma_0$ , the cross section for lepton production shown in the diagram of figure 5b, in the limit  $E_\psi \gg M_\psi$  where fragmentation dominates.

The general form of the cross section  $\sigma_0$  for lepton production is

$$\sigma_0 = \frac{1}{Flux} \int [dq][dp_{out}] (2\pi)^4 \delta^4(p_{in} - q - p_{out}) \sum |A_0|^2, \quad (23)$$

where  $q$ ,  $p_{in}$ , and  $p_{out}$  are the 4-momenta of the  $\ell^-$ , the incoming particles, and all other outgoing particles. Just as in the photon fragmentation calculation,  $[dq]$  and  $[dp_{out}]$  are the Lorentz invariant phase space for the lepton and the remaining outgoing particles, and  $Flux$  represents the incoming particle flux (which will cancel with the same quantity in the cross section  $\sigma_1$ ). The square of the amplitude  $A_0$  calculated from the Feynman diagram in figure 4b for  $\ell^-$  production, averaged over initial spins and summed over final spins, is

$$\sum |A_0|^2 = \text{tr}[\not{q} \Gamma \bar{\Gamma}] \quad (24)$$

where the Dirac matrix  $\Gamma$  is the matrix element for the production of a real lepton of momentum  $q$  for which the explicit form is not needed. The lepton mass  $m_\ell$  has been neglected since its 4-momentum  $q$  is taken to be large compared to  $m_\ell$ .

The general form of the cross section  $\sigma_1$  for the production of a lepton that subsequently fragments into a  $\psi$  is

$$\frac{1}{Flux} \int [dP][dp_-][dp_{out}] (2\pi)^4 \delta^4(p_{in} - P - p_- - p_{out}) \sum |A_1|^2, \quad (25)$$

where  $P$  is the  $\psi$  4-momentum, and everything else is as described after Eq. (23). The next step is to write the phase space in an iterated form, by introducing integrals over  $q = P + p_-$

the virtual lepton momentum, and  $s = q^2$  the invariant mass of the  $\psi - \ell^-$  system. Then the phase space expression becomes

$$\begin{aligned} & \int [dP][dp_-] (2\pi)^4 \delta^4(p_{in} - P - p_- - p_{out}) \\ &= \int \frac{ds}{2\pi} \int [dq] (2\pi)^4 \delta^4(p_{in} - q - p_{out}) \int [dP][dp_-] (2\pi)^4 \delta^4(q - P - p_-). \end{aligned} \quad (26)$$

The contribution that corresponds to the fragmentation of the lepton in the diagram of figure 5a comes from the region of phase space in which the  $\psi - \ell^-$  system has large momentum  $q$  compared to the  $\psi$  mass and small invariant mass  $s = q^2$  of order  $M_\psi^2$ . In a frame in which the virtual lepton has a 4-momentum  $q = (q_0, 0, 0, q_3)$ , the longitudinal momentum fraction of the  $\psi$  relative to the  $\psi - \ell^-$  system is  $z = (P_0 + P_3)/(q_0 + q_3)$  and its transverse momentum is  $\vec{P}_\perp = (P_1, P_2)$ . Expressing the phase space in terms of these variables and integrating over the 4-momentum  $p_-$  and over  $\vec{P}_\perp$ , the 2-body phase space reduces to [3]

$$\int [dP][dp_-] (2\pi)^4 \delta^4(q - P - p_-) = \frac{1}{8\pi} \int_0^1 dz \theta\left(s - \frac{M_\psi^2}{z}\right). \quad (27)$$

The lepton mass has been set to zero. An upper limit on the integral over the invariant mass  $s$  is introduced by requiring  $s < \mu^2$ , as discussed earlier.

The calculation of the lepton fragmentation function is simplest to do in the axial gauge, because only the diagram of figure 5a, where the lepton is produced and splits into a collinear lepton and  $\psi$ , needs to be considered. Other diagrams where both the lepton and  $\psi$  are produced separately from the vertex  $\Gamma$  are suppressed in this gauge. If the calculation were done in some other gauge these diagrams would need to be considered, but the resulting expression could be manipulated into the form below using Ward identities. The 4-vector  $N$  associated with axial gauge is chosen to be  $N = (1, 0, 0, -1)$ . The amplitude  $A_1$  calculated in this gauge can be reduced to

$$A_1 = e^2 g_\psi \epsilon_\beta(P)^* \frac{1}{s} (\bar{u}(p_-) \gamma_\alpha \not{q} \Gamma) \left( g^{\alpha\beta} - \frac{P^\alpha N^\beta + P^\beta N^\alpha}{P \cdot N} \right). \quad (28)$$

where  $\epsilon$  is the  $\psi$  polarization vector, and  $\Gamma$  is the Dirac matrix element for the production

of a virtual lepton with an invariant mass  $s$  on the order of the  $\psi$  mass. The explicit form of  $\Gamma$  is not needed.

The  $\psi$  4-momentum can be written as  $P^\mu = zq^\mu + P_\perp^\mu + (P_0q_3 - q_0P_3)/(q_0 + q_3)N^\mu$ . In the fragmentation region  $P_\perp^\mu = (0, \vec{P}_\perp, 0)$ , and  $P_0q_3 - q_0P_3$  are of order  $M_\psi$  while the virtual lepton momentum  $q$  is large compared to  $M_\psi$  so  $P \simeq zq$ . Note that in the fragmentation region both  $s = q^2$  and  $P \cdot q$  are of order  $M_\psi^2$ . Using these approximations and keeping only the leading order terms in  $q/M_\psi$  simplifies the square of the amplitude to

$$\sum |A_1|^2 = 32\pi^2\alpha^2 g_\psi^2 \left( \frac{(z-1)^2 + 1}{z} \frac{1}{s} - \frac{M_\psi^2}{s^2} \right) \text{tr}[q \Gamma \bar{\Gamma}]. \quad (29)$$

Integrating over  $s$  up to the scale  $\mu^2$  the lepton fragmentation probability is obtained by dividing the cross section  $\sigma_1$  by the cross section  $\sigma_0$ . The differences between  $\sigma_1$  and  $\sigma_0$  are due to the fact that  $q^2 \sim M_\psi^2$  in  $\sigma_1$ , while  $q^2 = 0$  in  $\sigma_0$ . These differences are on the order of  $M_\psi^2/E_\psi^2$  and in the fragmentation limit where  $E_\psi \gg M_\psi$  they can be neglected. The result is

$$\frac{\sigma_1}{\sigma_0} = \int_0^{\mu^2} ds \int_0^1 dz \theta(s - \frac{M_\psi^2}{z}) 2\alpha^2 g_\psi^2 \left( \frac{(z-1)^2 + 1}{z} \frac{1}{s} - \frac{M_\psi^2}{s^2} \right). \quad (30)$$

from this it is possible to extract the lepton fragmentation function

$$D_{\ell \rightarrow \psi}(z, \mu^2) = 2\alpha^2 g_\psi^2 \left[ \frac{(z-1)^2 + 1}{z} \log \frac{z\mu^2}{M_\psi^2} - z + \frac{M_\psi^2}{\mu^2} \right] \theta(z\mu^2 - M_\psi^2) \quad (31)$$

Note that the lepton fragmentation function is zero for values of  $z$  at which the production of a  $\psi$  is kinematically forbidden. Taking the limit  $\mu \gg M_\psi$  simplifies Eq. (31) to

$$D_{\ell \rightarrow \psi}(z, \mu^2) \approx 2\alpha^2 g_\psi^2 \left[ \frac{(z-1)^2 + 1}{z} \log \frac{z\mu^2}{M_\psi^2} - z \right]. \quad (32)$$

Just as in the calculation of the photon subprocess there is a price to be paid for this simplification. Eq. (32) does not have the correct threshold behavior at  $z = M_\psi^2/\mu^2$ , and it becomes negative for sufficiently small  $z$ . The fragmentation function Eq. (32) is shown at the scales  $\mu = 3M_\psi$  and  $\mu = 6M_\psi$  in figure 6. Note that there is a dramatic dependence

on the arbitrary factorization scale  $\mu$ . At the scale  $\mu = 6M_\psi$  the fragmentation function is much larger and peaks at a lower  $z$  value than at the scale  $\mu = 3M_\psi$ .

### Comparison with full calculation

The fragmentation contribution to the differential decay rate for  $Z^0 \rightarrow \psi + \ell^+ \ell^-$  is given by inserting  $P_{\gamma \rightarrow \psi}$  from Eq. (17),  $d\hat{\Gamma}/dE_\psi$  from Eq. (22), and  $D_{\ell \rightarrow \psi}$  from Eq. (32) into the factorization formula Eq. (9):

$$\frac{d\Gamma}{dE_\psi}(Z^0 \rightarrow \psi(E_\psi) + \ell^+ \ell^-) = 8\alpha^2 g_\psi^2 \frac{\hat{\Gamma}(Z^0 \rightarrow \ell^+ \ell^-)}{M_Z} \left[ \frac{(y-1)^2 + 1}{y} \log \frac{y^2 M_Z^2}{M_\psi^2} - 2y \right]. \quad (33)$$

Note that the  $\mu$ -dependence cancels exactly. It is now possible to verify that this agrees with the full calculation in the fragmentation limit Eq. (4).

Figure 7 compares the energy distribution of the full calculation Eq. (3) and the fragmentation calculation Eq. (33). It is clear from the graph that the fragmentation approximation breaks down for sufficiently small  $E_\psi$ . For  $E_\psi = 3M_\psi$  the difference between the two curves is less than 1%, while for  $E_\psi = 2M_\psi$  the difference is 5%. In practice there will often be a minimum energy below which detectors do not register particles. If this minimum energy is large enough then it is clear that the fragmentation approximation will give a result very close to the full calculation.

Figure 8 shows the energy distribution in the fragmentation limit separated into the lepton fragmentation contribution, the first term on the right hand side of Eq. (9), and the photon fragmentation contribution, the last term on the right hand side of Eq. (9). The contributions are shown at  $\mu = 3M_\psi$  and  $\mu = 6M_\psi$ . The relative contribution of the two production mechanisms depends dramatically on the factorization scale  $\mu$ , though the total, photon fragmentation plus lepton fragmentation is independent of  $\mu$ . At the scale  $\mu = 3M_\psi$  the contribution of the lepton fragmentation mechanism is negligible compared to the contribution from the photon fragmentation mechanism, while at the scale  $\mu = 6M_\psi$  both contributions are of the same order.

The analysis carried out in this paper applies equally to other heavy quark anti-quark states such as the  $\psi'$  and the  $\Upsilon$ . Unfortunately the fragmentation contribution to

$\Upsilon$  production is an order of magnitude smaller than the fragmentation contribution to  $\psi$  production. This is because the  $\Upsilon$ -photon coupling  $g_{\Upsilon}^2 = 6 \times 10^{-4}$  is so much smaller than the  $\psi$ -photon coupling  $g_{\psi}^2 = 8 \times 10^{-3}$ , and the  $\Upsilon$  mass is larger than the  $\psi$  mass.

### Conclusion

The process  $Z^0 \rightarrow \psi + \ell^+ \ell^-$  has been studied in the fragmentation limit  $M_Z \rightarrow \infty$  keeping  $E_{\psi}/M_Z$  fixed. In this limit the decay rate factors into the subprocess rates  $\hat{\Gamma}(Z^0 \rightarrow \ell^+ \ell^-)$  and  $\hat{\Gamma}(Z^0 \rightarrow \gamma + \ell^+ \ell^-)$ , convoluted with the electromagnetic fragmentation functions  $D_{\ell \rightarrow \psi}$  and  $D_{\gamma \rightarrow \psi}$ . The fragmentation function  $D_{\ell \rightarrow \psi}(z, \mu)$  for a lepton to split into  $\psi$ , the fragmentation probability  $P_{\gamma \rightarrow \psi}$  for a photon to split into  $\psi$ , and the subprocess  $\hat{\Gamma}(Z^0 \rightarrow \gamma + \ell^+ \ell^-)$  were calculated at lowest order in  $\alpha$ . The lepton fragmentation function was defined by imposing a cutoff on the invariant mass  $s$  of the lepton and  $\psi$  in the final state. This cutoff translated into limits on the phase space of the subprocess  $\hat{\Gamma}(Z^0 \rightarrow \gamma + \ell^+ \ell^-)$ . It was then explicitly shown that the  $\mu$ -dependence of the lepton fragmentation function canceled the  $\mu$ -dependence of the subprocess  $\hat{\Gamma}(Z^0 \rightarrow \gamma + \ell^+ \ell^-)$ . Comparison between the fragmentation calculation and the full calculation shows that the fragmentation approximation is accurate to within 5% at  $E_{\psi} = 2M_{\psi}$ , and becomes more accurate for  $\psi$  energies greater than this.

This work is supported in part by the U.S. Department of Energy, Division of High Energy Physics, under Grant DE-FG02-91-ER40684. I wish to thank E. Braaten for many helpful discussions, and his infinite patience. I also wish to thank the Fermilab theory group for their hospitality.

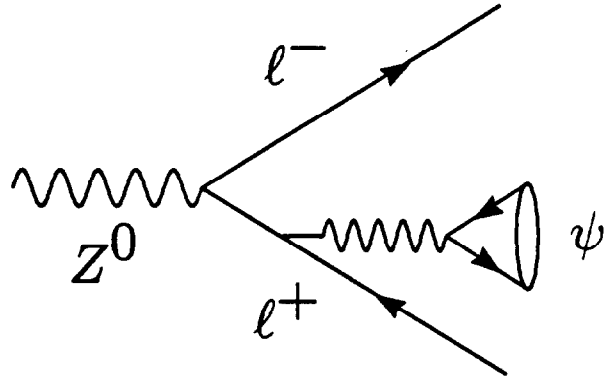
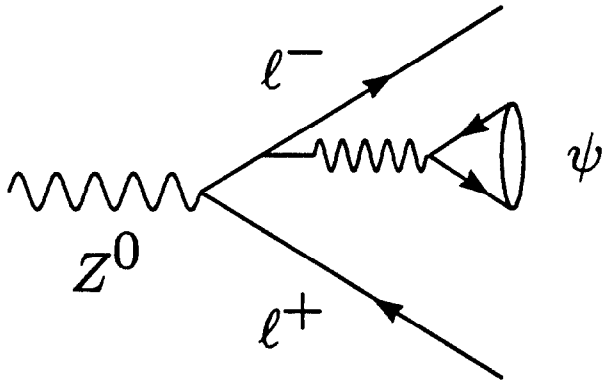
## References

- [1] J.C. Collins and G. Sterman, *Nucl. Phys.* **B185** 172 (1981); J.C. Collins and D.E. Soper, *Nucl. Phys.* **B194**, 445 (1982); G. Curci, W Furmanski and R. Petronzio, *Nucl. Phys.* **B175** (1980) 27.
- [2] E. Braaten and T.C. Yuan, *Phys. Rev. Lett.* **71**, 1673 (1993).
- [3] E. Braaten, K. Cheung and T.C. Yuan, *Phys. Rev.* **D48**, 4230 (1993).
- [4] E. Braaten, K. Cheung and T.C. Yuan, *Phys. Rev.* **D48**, R5049 (1993).
- [5] A.F. Falk, M. Luke, M.J. Savage, and M.B. Wise, *Phys. Lett.* **B312**, 486 (1993) and *Phys. Rev.* **D49**, 555 (1994).
- [6] C.-H. Chang and Y.-Q. Chen, *Phys. Lett.* **B284**, (1991) 142; *Phys. Rev.* **D46** 3845 (1992); Y.-Q. Chen, *Phys. Rev.* **D48**, 5158 (1993).
- [7] B.Guberina, J.H. Kühn, R.D.Peccei, and R. Rückl, *Nucl. Phys.* **B174**, 317 (1980).
- [8] S. Fleming, *Phys. Rev.* **D48**, R1914 (1993).
- [9] L. Bergström and R.W. Robinett, *Phys. Lett.* **B245**, 249 (1990).
- [10] J.H. Kühn and H. Schneider, *Phys. Rev.* **D24**, 2996 (1981) and *Z. Phys.* **C11**, 263 (1981).
- [11] K. Hagiwara, A.D. Martin and W.J. Stirling, *Phys. Lett.* **B267**, 527 (1991).

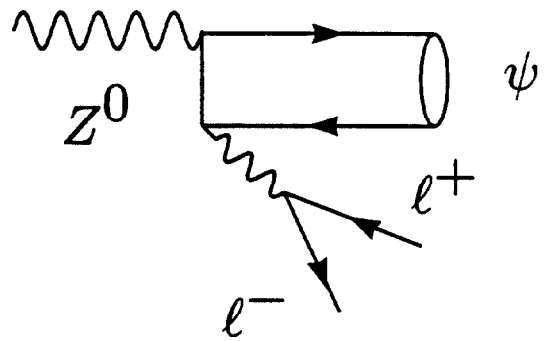
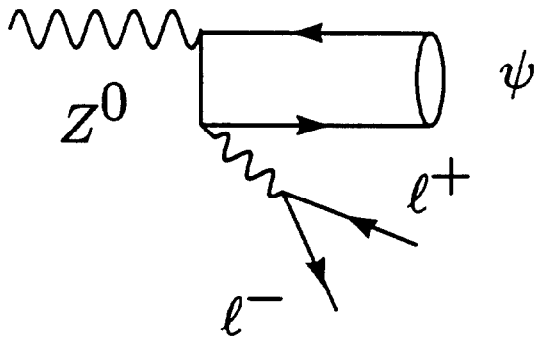
## Figure Captions

1. The Feynman diagrams for  $Z^0 \rightarrow \psi + \ell^+ \ell^-$  at leading order in  $\alpha$ . a) The two diagrams from which the fragmentation contribution can be isolated, and b) the two diagrams that may be neglected.
2. The two Feynman diagrams for  $Z^0 \rightarrow \psi \gamma$  at leading order in  $\alpha$ .

3. Feynman diagrams for a)  $\psi$  production by photon fragmentation, b) photon production. The shaded circle represents some general vertex that radiates the photon.
4. The two Feynman diagrams for  $Z^0 \rightarrow \gamma + \ell^+ \ell^-$  at leading order in  $\alpha$ .
5. Feynman diagrams for a)  $\psi$  production by lepton fragmentation, b) lepton production. The shaded circle represents some general vertex that radiates the lepton.
6. Lepton fragmentation function for  $\mu = 3M_\psi$  (solid) and  $\mu = 6M_\psi$  (dashes).
7. Energy distribution: the full calculation (solid), the fragmentation calculation (dashes).
8. Photon fragmentation (PF) and lepton fragmentation (LF) contributions to the energy distribution for  $\mu = 3M_\psi$  (solid) and  $\mu = 6M_\psi$  (dashes).

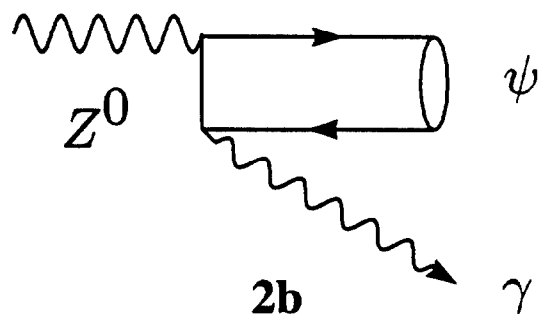
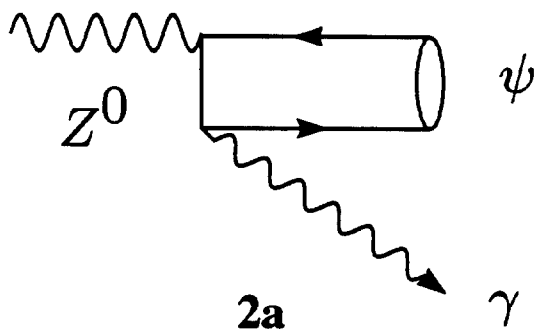


**1a**



**1b**

**Figure 1**



**2a**

**2b**

**Figure 2**

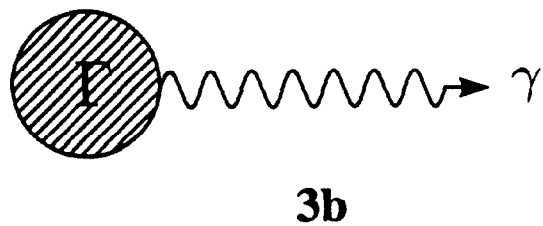
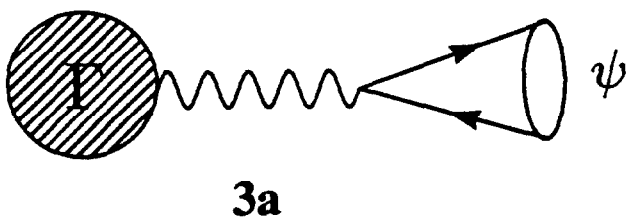


**Figure 3**

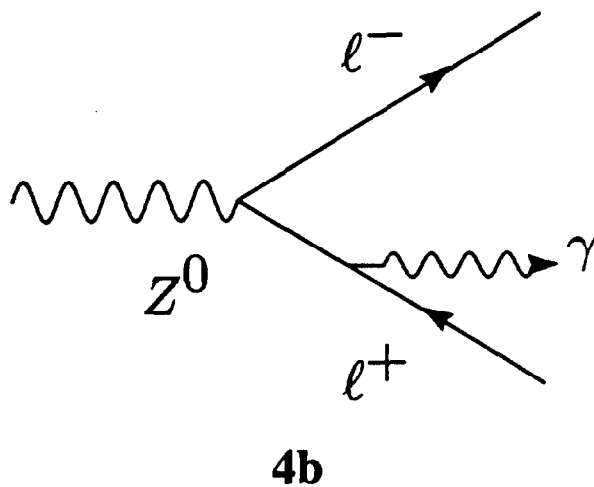
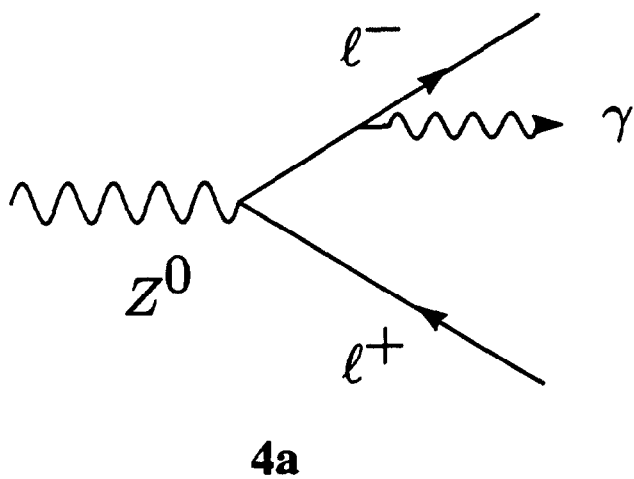


**Figure 4**

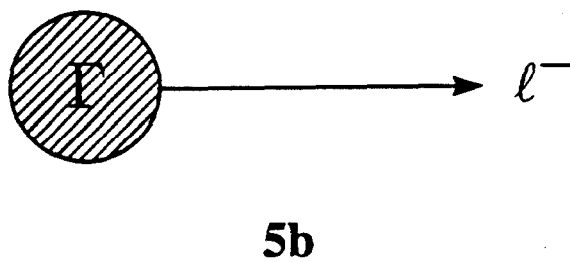
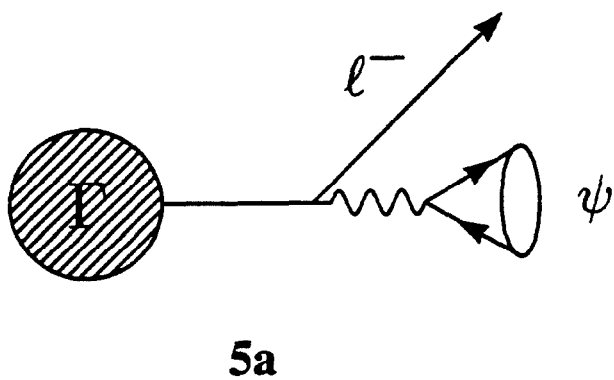


**Figure 5**

$D_{1 \rightarrow \psi}(z) (10^{-6})$

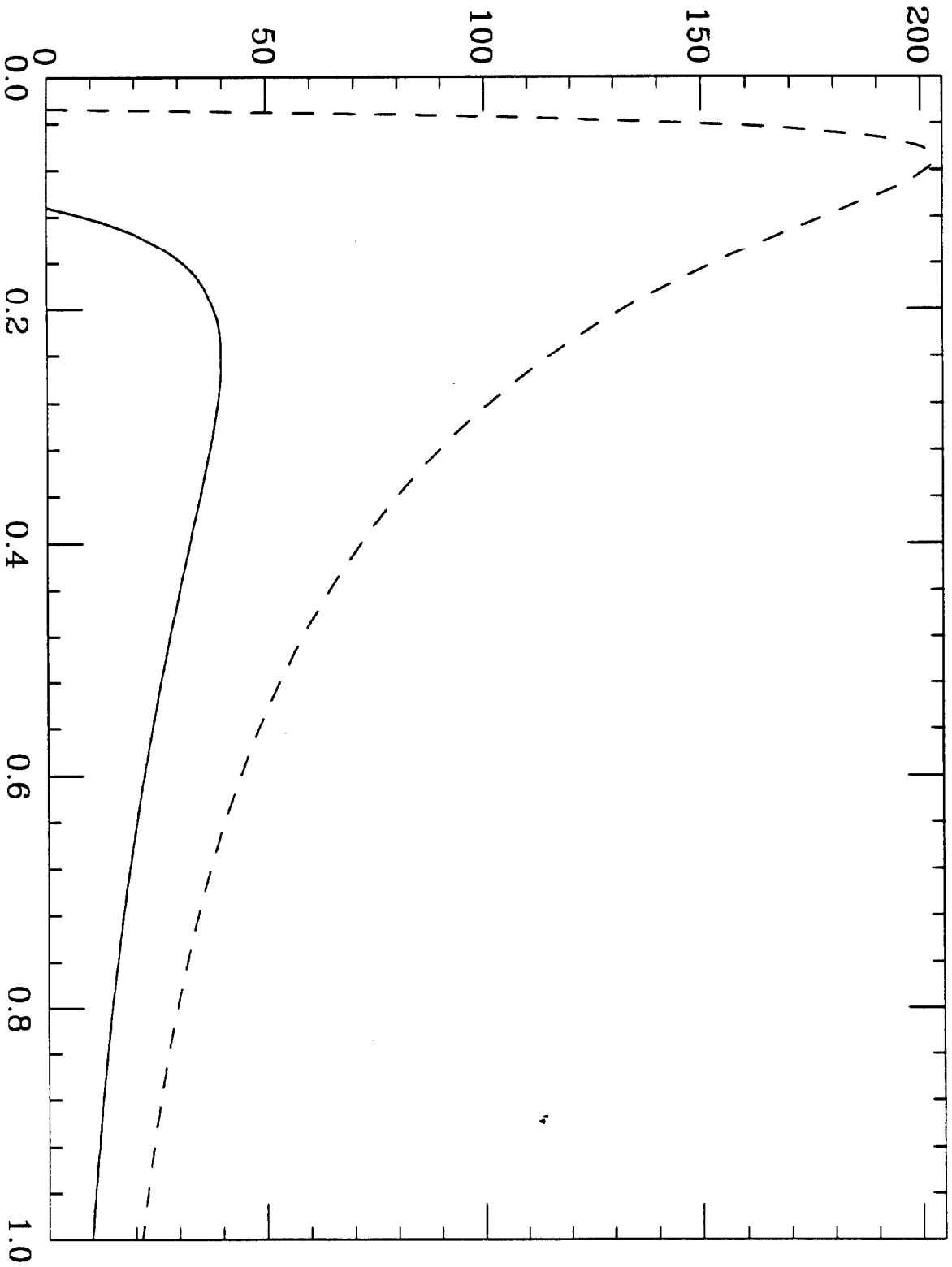
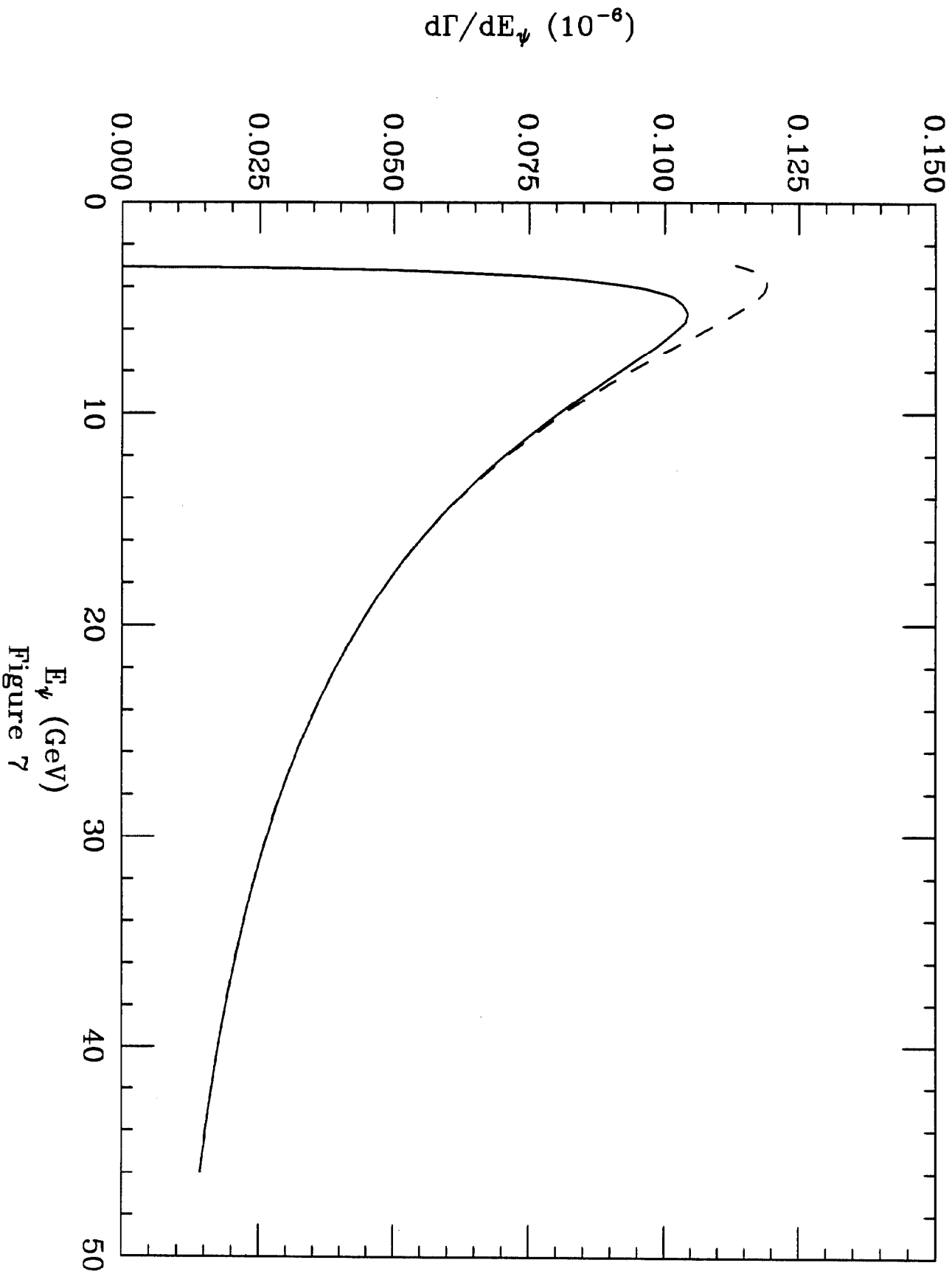


Figure 6



$E_\psi$  (GeV)  
Figure 7

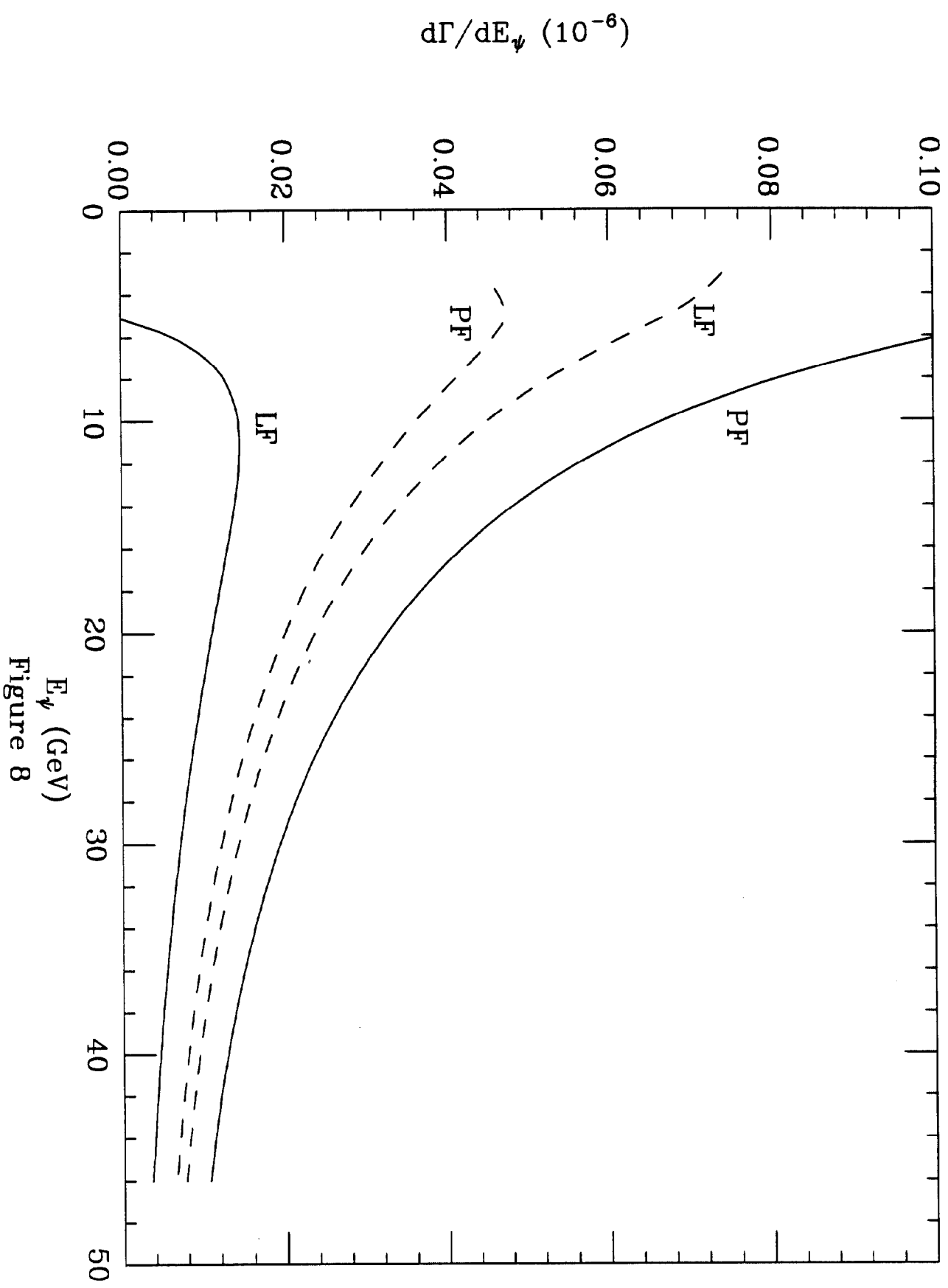


Figure 8